

See discussions, stats, and author profiles for this publication at: <https://www.researchgate.net/publication/314015990>

Raman spectroscopic characterization of light rare earth ions: La^{3+} , Ce^{3+} , Pr^{3+} , Nd^{3+} and Sm^{3+} – Hydration and ion pair formation.

Article in Dalton Transactions · March 2017

DOI: 10.1039/C7DT00008A

CITATIONS

8

READS

185

2 authors:



Wolfram Rudolph

Technische Universität Dresden

181 PUBLICATIONS 1,863 CITATIONS

[SEE PROFILE](#)



Gert Irmer

Technische Universität Bergakademie Freiberg

229 PUBLICATIONS 3,144 CITATIONS

[SEE PROFILE](#)

Some of the authors of this publication are also working on these related projects:



Hydration and ion pair formation in aqueous $\text{Ce}(\text{ClO}_4)_3(\text{aq})$. [View project](#)



polymer derived silicon carbide [View project](#)

PAPER



Cite this: *Dalton Trans.*, 2017, **46**, 4235

Raman spectroscopic characterization of light rare earth ions: La³⁺, Ce³⁺, Pr³⁺, Nd³⁺ and Sm³⁺ – hydration and ion pair formation†

Wolfram W. Rudolph^{*a} and Gert Irmer^b

Raman spectra of aqueous La³⁺, Ce³⁺, Pr³⁺, Nd³⁺ and Sm³⁺ – perchlorate solutions were measured and weak strongly polarized Raman bands were detected at 343 cm⁻¹, 344 cm⁻¹, 347 cm⁻¹, 352 cm⁻¹ and 363 cm⁻¹, respectively. The full width at half height for these bands is quite broad (~50 cm⁻¹) in the isotropic spectrum and the band width increases with increasing solute concentration. The polarized Raman bands were assigned to the breathing modes of the nona-aqua ions of the mentioned rare earth ions. Published structural results confirmed that these ions exist as nona-hydrates in aqueous solutions [Ln(H₂O)₉]³⁺. The Ln–O bond distances of these rare earth ions correlate well with the band positions of the nona-aqua ions [Ln(OH₂)₉]³⁺ (Ln = La³⁺, Ce³⁺, Pr³⁺, Nd³⁺ and Sm³⁺) and the force constants were calculated for these breathing modes. The strength of the force constants increase with decreasing the Ln–O bond distances (La–O > Ce–O > Pr–O > Nd–O > Sm–O). While the fully hydrated ions are stable in dilute perchlorate solutions (~0.2 mol L⁻¹), in concentrated perchlorate solutions outer-sphere ion pairs and contact ion pairs are formed (C > 1.5 mol L⁻¹). In a hydrate melt at 161 °C of Ce(ClO₄)₃ plus 6H₂O, the contact ion pairs are the dominate species. The Raman bands of the ligated perchlorate and the Ce–O breathing mode of the partially hydrated ion pair at 326 cm⁻¹ were measured and characterized. In cerium chloride solutions chloro-complex formation was detected over the measured concentration range from 0.270–2.167 mol L⁻¹. The chloro-complexes in CeCl₃(aq) are weak and diminish rapidly with dilution and disappear at a concentration <0.1 mol L⁻¹. In a CeCl₃ solution, with additional HCl, a series of chloro-complex species of the type [Ce(OH₂)_{9-n}Cl_n]⁺³⁻ⁿ (n = 1, 2) were detected.

Received 2nd January 2017,
Accepted 24th February 2017

DOI: 10.1039/c7dt00008a

rsc.li/dalton

1. Introduction

In aqueous solution, the light rare earth ions of lanthanum, cerium, praseodymium, neodymium and samarium exist in the trivalent state¹ although cerium also exists in the tetravalent state, Ce⁴⁺(aq) with its stability kinetically controlled.² The focus here, however, is on the trivalent ions. The lanthanide ions, Ln³⁺, with their high charge to radius ratio are strongly hydrated judging from their hydration energy.^{3,4} The light rare earth ions mentioned possess nine water molecules in their first sphere and have the configuration of a tricapped trigonal prism (TTP) with D₃ symmetry. The O-atoms of the three waters in the equatorial plane (capping position) are separated from the Ln³⁺ ions by a slightly longer bond distance, while six

water molecules at the vertices of the trigonal prism have slightly shorter ones.^{5,6} The hydration numbers of Ln³⁺ ions in aqueous solution were determined by X-ray diffraction (XRD)⁷ and extended X-ray absorption fine structure (EXAFS)^{5,8} methods.

In addition to the experimental work, computer simulations significantly contributed to clarifying the details of the structure and dynamics of the waters in the first hydration shell of Ln³⁺ (ref. 9 and 10) and have confirmed the nona-hydrate coordination for the mentioned rare earth ions from La³⁺ to Sm³⁺.

X-ray scattering investigation and EXAFS studies were applied at quite different concentration levels. While XRD measurements⁷ are carried out in concentrated solutions (moles per L), EXAFS studies^{5,6,8} are measured on dilute or moderately concentrated solutions. The high concentrations, however, pose a challenge because in aqueous trivalent metal ion solutions complex formation is common and therefore the Ln³⁺(aq) ions may form complexes. The fully hydrated ions are then in equilibrium with partially hydrated ions which contain the ligated anion. Rare earth ions easily form complexes/ion

^aMedizinische Fakultät der TU Dresden, Institut für Virologie im MTZ, Fiedlerstr. 42, 01307 Dresden, Germany. E-mail: Wolfram.Rudolph@tu-dresden.de

^bTechnische Universität Bergakademie Freiberg, Institut für Theoretische Physik, Leipziger Str. 23, 09596 Freiberg, Germany

†Electronic supplementary information (ESI) available. See DOI: 10.1039/c7dt00008a

pairs with common ions such as chloride, sulfate and nitrate. Perchlorate, however, acts as a non-complexing anion but at high concentrations may form ion pairs. Perchlorato-complexes in solution have been described previously, however, the views expressed were controversial.^{11–13}

Vibrational spectroscopy, especially Raman spectroscopy, is frequently applied to characterize hydrated metal ions and related species in aqueous solution. It is especially useful to characterize the species formed at the molecular level such as hydrated ions, ion pairs between metal ions and anions or hydrolysis. Raman scattering measurements on aqueous $\text{Ln}^{3+}(\text{aq})$ should allow, in principle, the characterization of the solution structure in greater detail. However, aqueous Ln^{3+} solutions at high concentrations in the vitreous state have been investigated by Raman spectroscopy in only a few studies (e.g. ref. 14). Due to the limitations of Raman spectroscopy in the past, the spectra in the low frequency range were of low quality and Nd^{3+} salt solutions were not measured due to their lilac color.¹⁴ It has been shown on a variety of aqueous metal salt solutions that for meaningful Raman spectroscopic analysis, R -normalized spectra were necessary in the terahertz frequency range^{15,16} in order to account for the Bose–Einstein correction and the scattering factor.¹⁷

The present study was undertaken to characterize the hydration and speciation in aqueous Ce^{3+} , Pr^{3+} , Nd^{3+} and Sm^{3+} perchlorate solutions, including La^{3+} which was studied recently.¹⁸ For this purpose, Ce^{3+} , Pr^{3+} , Nd^{3+} and Sm^{3+} perchlorate solutions were measured over broad concentration ranges and down to the terahertz frequency region. The $\text{Ce}(\text{ClO}_4)_3$ solutions in heavy water were measured in order to characterize the vibrational isotope effect changing from $[\text{Ce}(\text{H}_2\text{O})_9]^{3+}$ to $[\text{Ce}(\text{D}_2\text{O})_9]^{3+}$.

In chloride solutions, however, it was shown that these anions readily form complexes with a variety of di- and trivalent metal ions^{16,18} and the question arises as to whether these complexes also occur in $\text{Ce}^{3+}(\text{aq})$. Therefore, exemplary for the other rare earth ions, aqueous CeCl_3 solutions were measured at varying concentrations to answer this question. Recently, inner-sphere chloro-complexes were verified in aqueous LaCl_3 solutions using Raman spectroscopy.¹⁸

The following aqueous lanthanide solution systems were measured Raman spectroscopically at 22 °C: $\text{Ce}(\text{ClO}_4)_3$, $\text{Pr}(\text{ClO}_4)_3$, $\text{Nd}(\text{ClO}_4)_3$, and $\text{Sm}(\text{ClO}_4)_3$. (The $\text{La}(\text{ClO}_4)_3$ solutions were previously measured.¹⁸) Specifically, we were interested in the vibrational characterization of the Ln–O stretching modes of the nona-hydrate of the fully hydrated ions, $[\text{Ln}(\text{OH}_2)_9]^{3+}$ as a function of solute concentration and the possible formation of ion pairs between Ln^{3+} ions and the perchlorate ion. The concentration dependence of $\text{Ce}(\text{ClO}_4)_3$ solution spectra were measured from the dilute solutions to concentrated. Furthermore, a $\text{Ce}(\text{ClO}_4)_3$ hydrate melt at 161 °C ($\text{Ce}(\text{ClO}_4)_3$ plus $6\text{H}_2\text{O}$) was measured and the bands characterized.

The influence of chloride on the fully hydrated $\text{Ln}^{3+}(\text{aq})$ was studied exemplarily on aqueous CeCl_3 solutions. For this purpose, CeCl_3 solutions and a CeCl_3 solution with additional HCl were measured.

2. Experimental details and data analysis

2.1. Preparation of solutions

The rare earth ion concentrations of all solutions were analysed by complexometric titration,¹⁹ the solution densities determined with a pycnometer at 22 °C and the molar ratios of water per salt calculated (R_w -values). For Raman spectroscopic measurements, the solutions were filtered through a fine sintered glass frit (1–1.6 μm pore size). The solutions showed no Tyndall effect and were “optically empty”.²⁰

The preparation and characterization of lanthanum perchlorate solutions at various concentrations, from dilute to highly concentrated were described earlier.¹⁸

Cerium perchlorate solutions were prepared from $\text{Ce}(\text{ClO}_4)_3 \cdot 6\text{H}_2\text{O}$ (Alfa-Aesar, 99.9%) dissolved with ultrapure water (PureLab Plus, Ultra-pure Water Purification Systems). A concentrated $\text{Ce}(\text{ClO}_4)_3$ solution was prepared at 3.118 mol L^{-1} ($R_w = 11.68$). This solution was acidified with a slight amount of HClO_4 and a pH value at ~ 1.8 was measured. From this stock solution, the following dilution series was prepared: 1.886 mol L^{-1} ($R_w = 22.03$), 0.942 mol L^{-1} ($R_w = 51.47$), 0.404 mol L^{-1} ($R_w = 129.14$) and 0.202 mol L^{-1} ($R_w = 268.74$). The solutions were analysed for dissolved chloride with a 5% AgNO_3 solution and the absence of a white AgCl precipitate was proof that the stock solution was free of Cl^- . (This is important because chloride forms complexes with Ce^{3+} albeit weak.) Crystalline $\text{Ce}(\text{ClO}_4)_3 \cdot 6\text{H}_2\text{O}$ was fused in a quartz cuvette (Hellma Analytics, Müllheim, Germany) for temperature dependent measurements.

Two $\text{Ce}(\text{ClO}_4)_3$ solutions in heavy water were prepared from a $\text{Ce}(\text{ClO}_4)_3$ stock solution in D_2O (99.9 atom% D; Sigma-Aldrich) at 2.562 mol L^{-1} and 1.281 mol L^{-1} . The deuteration degree in the solution was determined at 97% D.

CeCl_3 solutions were prepared from $\text{CeCl}_3 \cdot 7\text{H}_2\text{O}$ (Sigma-Aldrich, 99.5%) and ultrapure water (PureLab Plus, Ultra-pure Water Purification Systems) by weight 2.167 mol L^{-1} ($R_w = 23.61$), 1.083 mol L^{-1} ($R_w = 49.23$) and 0.270 mol L^{-1} ($R_w = 203.1$). Furthermore, a solution with an excess of HCl was prepared ($\text{CeCl}_3 + \text{HCl}$) at 1.678 mol L^{-1} CeCl_3 and an additional 4.012 mol L^{-1} HCl with a $\text{Ce}^{3+}(\text{aq}) : \text{Cl}^-(\text{aq})$ ratio at 1 : 5.69. A 4.090 mol L^{-1} aqueous HCl solution was prepared from a concentrated HCl stock solution and its HCl concentration checked by titration.

$\text{Pr}(\text{ClO}_4)_3$ and $\text{Nd}(\text{ClO}_4)_3$ stock solutions were commercial products from Alfa-Aesar at 50 wt%, Reagent Grade (99.9%). Dilute solutions were prepared by weight with ultrapure water. Two $\text{Pr}(\text{ClO}_4)_3$ solutions were prepared at 0.89 and 0.317 mol L^{-1} and two $\text{Nd}(\text{ClO}_4)_3$ solutions at 0.793 and 0.256 mol L^{-1} . These solutions contained a slight excess of HClO_4 and the solutions reacted therefore quite acidic (pH value < 1.5).

A 2.171 mol L^{-1} $\text{Sm}(\text{ClO}_4)_3$ stock solution ($R_w = 21.04$) was prepared from samarium(III) oxide (Aldrich, 99.9%) with a 8.2 mol L^{-1} HClO_4 by weight. Two dilute solutions were prepared from the stock solution with ultrapure water at

1.085 mol L⁻¹ ($R_w = 45.59$) and 0.274 mol L⁻¹ ($R_w = 199.91$). These solutions contained a slight excess of HClO₄ and the solutions reacted therefore quite acidic (pH value <1.5).

To further characterize the rare earth solutions UV-VIS (ultraviolet-visible) – absorption spectra were measured on Ce(ClO₄)₃, Pr(ClO₄)₃ and Nd(ClO₄)₃ solutions. La(ClO₄)₃(aq) Ce(ClO₄)₃(aq) are colourless. However, Ce³⁺(aq) shows five characteristic UV absorption bands.²¹ Pr(ClO₄)₃ and Nd(ClO₄)₃ – solutions are quite strongly coloured. The UV-VIS absorption spectra were measured from 190 nm to 1100 nm in 1 cm quartz cuvettes (Hellma Analytics; Müllheim/Germany) with the UV-visible spectrophotometer Evolution 201 from Thermo Fischer. The spectral resolution was set at 1 nm. Ce(ClO₄)₃ solutions were measured from 190–400 nm (UV absorption). The UV/UV-vis spectra (see Fig. S1A–C, ESI†) compare favourably with the ones given in the literature²² and shall not be further discussed.

2.2. Spectroscopic measurements

Raman spectra were measured in the macro chamber of the T 64000 Raman spectrometer from Jobin Yvon in a 90° scattering geometry at 22 °C. These measurements have been described elsewhere.^{14,16} A quartz cuvette from Hellma Analytics (Müllheim, Germany) with a 10 mm path length and a volume 1000 μL was used. Briefly, the spectra were excited with the 487.987 nm or the 514.532 nm line of an Ar⁺ laser at a power level of 1100 mW at the sample. The spectral resolution at 950 cm⁻¹ was 2.90 cm⁻¹ using the 487.987 nm excitation line and 2.61 cm⁻¹ using the one at 514.532 nm. For the transparent solution of La³⁺ and Ce³⁺ both excitation wavelength were used. Pr(ClO₄)₃ and Sm(ClO₄)₃ solutions were measured with the 514.532 nm Ar⁺ line. Nd(ClO₄)₃ solutions were excited with the 487.987 nm Ar⁺ line and only the most dilute solution could be measured because the concentrated ones absorbed too strongly despite the absorption gap at 488 nm of its UV-vis spectrum. The laser beam was focused on the sample by a laser objective. The Gaussian beam width was *ca.* 38 μm at the focal plane. The length of the laser inside the sample was *ca.* 10 mm but only 2 mm of the focused laser beam was transferred into the spectrometer. After passing the spectrometer in subtractive mode, with gratings of 1800 grooves per mm, the scattered light was detected with a cooled CCD detector. I_{VV} and I_{VH} spectra were obtained with fixed polarization of the laser beam by rotating the polarizer at 90° between the sample and the entrance slit to give the scattering geometries:

$$I_{VV} = I(Y[ZZ]X) = 45\alpha^2 + 4\gamma^2 \quad (1)$$

and

$$I_{VH} = I(Y[ZY]X) = 3\gamma^2. \quad (2)$$

The isotropic spectrum, I_{iso} was then constructed:

$$I_{iso} = I_{VV} - 4/3 \times I_{VH}. \quad (3)$$

The polarization degree of the Raman bands, ρ ($\rho = I_{VH}/I_{VV}$) was determined using a polarizer and adjusted if necessary

before each measuring cycle using CCl₄. A detailed account of this procedure may be found in ref. 16.

In order to obtain spectra defined as $R(\bar{\nu})$ which are independent of the excitation wavenumber ν_L , the measured Stokes intensity should be corrected for the scattering factor $(\nu_L - \bar{\nu})^3$. In the case of counting methods used, the measured count rates were corrected with the factor $(\nu_L - \bar{\nu})^3$. The spectra were further corrected for the Bose–Einstein temperature factor, $B = [1 - \exp(-h\bar{\nu}c/kT)]$ and the frequency factor, $\bar{\nu}$, to give the so called reduced spectrum, $R(\bar{\nu})$. It is also possible to calculate the isotropic spectrum in R -format from the corrected R_{VV} and R_{VH} spectra according to eqn (4):

$$R(\bar{\nu})_{iso} = R(\bar{\nu})_{VV} - 4/3R(\bar{\nu})_{VH}. \quad (4)$$

In the low wavenumber region, the $I(\bar{\nu})$ and $R_Q(\bar{\nu})$ spectra are significantly different and only the spectra in R -format are presented. The advantages of using isotropic R -spectra is that the baseline is almost flat in the terahertz region allowing relatively unperturbed observation of the presence of any weak modes.¹⁶

Temperature dependent Raman measurements were carried out in a sealable fused quartz cuvette, 10 × 10 mm, with 3.5 mL volume from Hellma (Müllheim, Germany) using a home-built oven. The oven and the experimental setup have been described in detail in ref. 23.

3. Results and discussion

3.1. Raman spectra on aqueous Ln(ClO₄)₃ solutions (Ln = La³⁺, Ce³⁺, Pr³⁺, Nd³⁺ and Sm³⁺)

The perchlorate spectrum, ClO₄⁻(aq). The Raman spectrum of the perchlorate ion in hydrated form (dilute NaClO₄(aq)) has been well characterized and only a brief description shall be given ref. 15, 16 and 18. The ClO₄⁻ ion possesses T_d symmetry and has nine modes of internal vibrations spanning the representation $\Gamma_{vib}(T_d) = a_1(Ra) + e(Ra) + 2f_2(Ra, i.r.)$. All normal modes are Raman active, but in *i.r.* only the f_2 modes are allowed. The $\nu_1(a_1)$ ClO₄⁻ band, centred at 931.5 cm⁻¹, is totally polarized ($\rho = 0.005$) whereas $\nu_3(f_2)$ ClO₄⁻, centred at 1106 cm⁻¹, is depolarized as are the deformation modes $\nu_4(f_2)$ ClO₄⁻ at 628 cm⁻¹ and $\nu_2(e)$ ClO₄⁻ at 462 cm⁻¹.¹⁵ In dilute aqueous NaClO₄ solutions, the spectrum of ClO₄⁻(aq) shows no sign of contact ion pairs or outer-sphere ion pairs; the $\nu_1(a_1)$ ClO₄⁻ band at 931.5 cm⁻¹ is quite narrow with a full width at half height (fwhh) = 7.2 cm⁻¹. However, the $\nu_1(a_1)$ ClO₄⁻ band shows an intrinsic low frequency shoulder at 923 cm⁻¹ ‡ and this feature is due to Fermi resonance of the overtone of $\nu_2(e)$ ClO₄⁻, $2 \times \nu_2(e) = 923$ cm⁻¹ with $\nu_1(a_1)$ ClO₄⁻. This fact is relevant to the interpretation of the peculiar band

‡ This band is due to the Fermi resonance of the overtone of $\nu_2(e)$ ClO₄⁻ band at 462 cm⁻¹ with $\nu_1(a_1)$ ClO₄⁻. In NH₄ClO₄(cr) the bands are very narrow and the $\nu_1(a_1)$ ClO₄⁻ band which is only 2.5 cm⁻¹ in width shows a well separated overtone $2 \times \nu_2(e)$ at 923 cm⁻¹. The Raman spectrum of crystalline NH₄ClO₄(cr) is given in Fig. S2, ESI†

shape of the $\nu_1(a_1)$ ClO_4^- mode. The antisymmetric stretching mode, $\nu_3(f_2)$ ClO_4^- , is much weaker in intensity than $\nu_1(a_1)$ and it appears at 1106 cm^{-1} with a $\text{fwhh} = 65\text{ cm}^{-1}$.

The Raman spectra of $\text{La}(\text{ClO}_4)_3(\text{aq})$, $\text{Ce}(\text{ClO}_4)_3(\text{aq})$, $\text{Pr}(\text{ClO}_4)_3(\text{aq})$, $\text{Nd}(\text{ClO}_4)_3(\text{aq})$ and $\text{Sm}(\text{ClO}_4)_3(\text{aq})$. The Raman spectra of aqueous $\text{La}(\text{ClO}_4)_3$ solutions have been reported recently and a strongly polarized band in $\text{La}(\text{ClO}_4)_3(\text{aq})$ was observed at 343 cm^{-1} .¹⁸ Here, only the Raman spectra on aqueous $\text{Ce}(\text{ClO}_4)_3$, $\text{Pr}(\text{ClO}_4)_3$, $\text{Nd}(\text{ClO}_4)_3$ and $\text{Sm}(\text{ClO}_4)_3$ solutions shall be presented. The Fig. 1 shows an overview spectrum of an aqueous $\text{Ce}(\text{ClO}_4)_3$ solution at 0.202 mol L^{-1} representative of the last three solutions while the Raman spectra of the $\text{Pr}(\text{ClO}_4)_3$, $\text{Nd}(\text{ClO}_4)_3$ and $\text{Sm}(\text{ClO}_4)_3$ solutions are given in Fig. S3–S5, ESI† respectively. The Raman scattering profiles in Fig. 1, from 40 – 1430 cm^{-1} , show the $\text{ClO}_4^-(\text{aq})$ bands and in addition a broad, weak polarized mode at 344 cm^{-1} which does not occur in dilute $\text{NaClO}_4(\text{aq})$. Therefore, the band at 344 cm^{-1} has to be assigned to the ν_1 CeO_9 breathing mode of the $[\text{Ce}(\text{H}_2\text{O})_9]^{3+}$ species in analogy to the assignment in the $\text{La}(\text{ClO}_4)_3(\text{aq})$ system.¹⁸

In Fig. 2, the concentration dependence of the ν_1 CeO_9 breathing mode in $\text{Ce}(\text{ClO}_4)_3$ solutions from 0.202 mol L^{-1} ($R_w = 268.74$) to 1.886 mol L^{-1} ($R_w = 22.03$) is given. The ν_1 Ce–O breathing mode appears at 344 cm^{-1} at the lowest concentration and shifts $\sim 2\text{ cm}^{-1}$ to lower wavenumbers with increasing concentration. Furthermore, the fwhh also increases with increasing solute concentration from 50 cm^{-1} for the 0.202 mol L^{-1} solution to 56 cm^{-1} for the 1.886 mol L^{-1} solution (Fig. 2). This slight change in band parameters of ν_1 CeO_9 breathing mode may be due to ion pair formation in concentrated solutions. This ion-pairing effect will be discussed below. The integrated band intensity of ν_1 CeO_9 breathing mode rises linearly with the solution concentration (Fig. S6, ESI†).

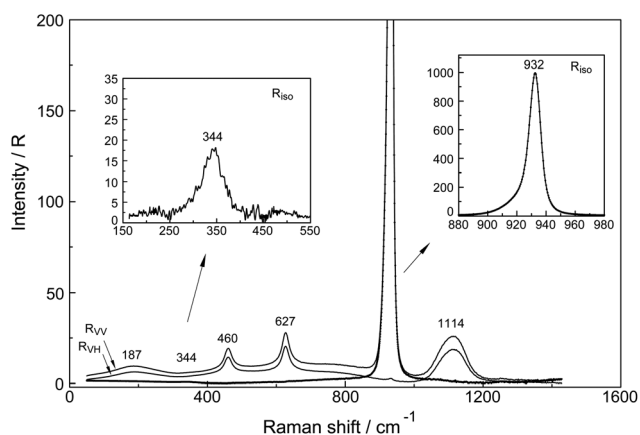


Fig. 1 Raman spectrum (R_{VV} , R_{VH} as indicated by arrows and R_{iso} with slightly thicker line) of a 0.202 mol L^{-1} $\text{Ce}(\text{ClO}_4)_3$ from 40 – 1430 cm^{-1} . The band at 344 cm^{-1} represents the breathing mode of CeO_9 skeleton of $[\text{Ce}(\text{OH}_2)_9]^{3+}$ and the strong band 460 cm^{-1} , 627 cm^{-1} , 932 cm^{-1} and 1114 cm^{-1} are due to $\text{ClO}_4^-(\text{aq})$. The left inset shows the isotropic scattering of the Ce–O breathing mode of $[\text{Ce}(\text{OH}_2)_9]^{3+}$ in greater detail and the right inset shows the isotropic scattering profile of the $\nu_1(a_1)$ Cl–O stretching band.

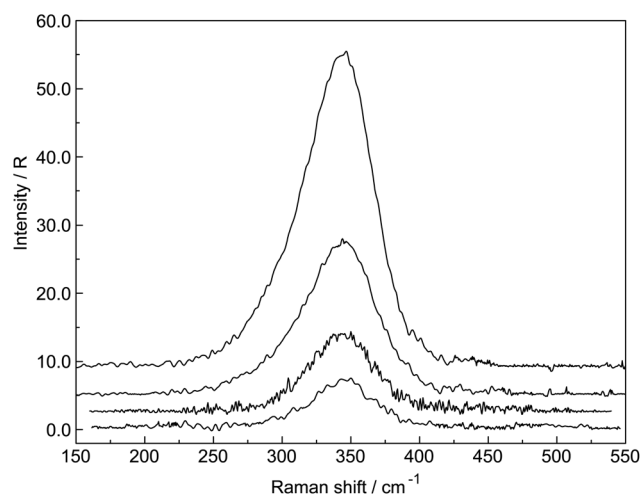


Fig. 2 Concentration plot of isotropic Raman spectra of $\text{Ce}(\text{ClO}_4)_3(\text{aq})$ (baseline corrected). From bottom to top: 0.202 , 0.404 , 0.942 and 1.889 mol L^{-1} cerium perchlorate in aqueous solution.

The effect of deuteration on the CeO_9 skeleton mode of $[\text{Ce}(\text{OD}_2)_9]^{3+}$ was studied in $\text{Ce}(\text{ClO}_4)_3\text{-D}_2\text{O}$ solutions and resulted in a shift of the Ce–O mode down to 326 cm^{-1} . The shift of ν_1 on deuteration is given by $\nu'_1 = \nu_1[m(\text{H}_2\text{O})/m(\text{D}_2\text{O})]^{1/2} = 344\sqrt{(18.02/20.03)} = 326.3\text{ cm}^{-1}$. (The water and heavy water molecules are viewed as point masses.) Raman spectra of $\text{Ce}(\text{ClO}_4)_3$ solutions in D_2O at 1.281 and a 2.562 mol L^{-1} are presented in Fig. S7, ESI†.

In addition to the isotropic mode, ν_1 CeO_9 of $[\text{Ce}(\text{OH}_2)_9]^{3+}$ at 344 cm^{-1} ($\text{fwhh} = 50 \pm 2\text{ cm}^{-1}$) a very weak, broad mode centered at $165 \pm 10\text{ cm}^{-1}$ can be observed in aqueous $\text{Ce}(\text{ClO}_4)_3$ solution (isotropic Raman scattering). This isotropic band is assigned to a restricted translational mode of the weakly H-bonded water molecules ($\text{O-H}\cdots\text{OClO}_3^-$). The mode is strongly anion and concentration dependent.^{15,16} The influence of the ClO_4^- on the water spectrum has been discussed in a recent study on aqueous $\text{La}(\text{ClO}_4)_3$ solutions¹⁸ and the Raman spectra of the O–H stretching region and the H_2O bending region of the solutions are given in Fig. S8, ESI† without further discussion.

In the Raman spectra of the $\text{Pr}(\text{ClO}_4)_3$, $\text{Nd}(\text{ClO}_4)_3$ and $\text{Sm}(\text{ClO}_4)_3$ solutions (Fig. S3–S5, ESI†), strongly polarized bands were observed at 347 , 352 cm^{-1} and 363 cm^{-1} , respectively, which cannot be found in the hydrated $\text{ClO}_4^-(\text{aq})$ spectrum. Again, several concentrations of the $\text{Pr}(\text{ClO}_4)_3$, $\text{Nd}(\text{ClO}_4)_3$ and $\text{Sm}(\text{ClO}_4)_3(\text{aq})$ solutions were measured. The peak positions for the ν_1 LnO_9 breathing modes of $[\text{La}(\text{OH}_2)_9]^{3+}$ (ref. 18), $[\text{Ce}(\text{OH}_2)_9]^{3+}$, $[\text{Pr}(\text{OH}_2)_9]^{3+}$, $[\text{Nd}(\text{OH}_2)_9]^{3+}$ and $[\text{Sm}(\text{OH}_2)_9]^{3+}$ are given in Table 1. Force constant calculations for the ν_1 LnO_9 breathing modes of this species, applying a simple model, have been carried out according to eqn (5):

$$k_{\text{M-O}} = 4\pi^2 c^2 \tilde{\nu}_1^2 N^{-1} A_L \quad (5)$$

with c , the velocity of light, $\tilde{\nu}_1$ the wavenumber of the totally symmetric mode, N the Avogadro number and A_L the mole-

Table 1 Vibrational frequencies, Ln–O bond distances⁹ and calculated force constant, $k_{\text{Ln-O}}$ for the $[\text{Ln}(\text{OH}_2)_9]^{3+}$ species of La^{3+} , Ce^{3+} , Pr^{3+} , Nd^{3+} and Sm^{3+} at 22 °C

$[\text{Ln}(\text{OH}_2)_9]^{3+}$	ν_1 Ln–O/cm ⁻¹	Ln–O/Å	$k_{\text{Ln-O}}/\text{Nm}^{-1}$
La^{3+}	343	2.585	124.88
Ce^{3+}	344	2.565	125.60
Pr^{3+}	347	2.540	127.80
Nd^{3+}	352	2.520	131.51
Sm^{3+}	363	2.490	139.86

cular weight of the ligand. The force constants, $k_{\text{Ln-O}}$, calculated for the measured ν_1 breathing modes are given in Table 1 together with the corresponding Ln³⁺–O bond distances.⁹ The force constants increase from La^{3+} , Ce^{3+} , Pr^{3+} , Nd^{3+} to Sm^{3+} in the same order as the corresponding Ln–O bond distances decrease.

Recently, Lutz *et al.*²⁴ computed the Ce–O stretching mode at 354 cm⁻¹ and compared their result with the band position measured in the glassy state of Ce³⁺-nitrate at 359 cm⁻¹ (ref. 13) and stated an “excellent agreement with experimental results”.²⁴ However, the peak position of the ν_1 CeO₉ breathing mode is 15 cm⁻¹ higher than our value at 344 cm⁻¹. Kanno and Hiraishi¹⁴ measured rare earth nitrate solutions including Ce³⁺-nitrate in vitreous state at a high concentration. It is known, that nitrates form nitrate-complexes especially at such high concentrations.¹⁴ From the Ce–O mode given in ref. 14 Lutz *et al.*²⁴ calculated the force constant for the ν_1 breathing mode of the $[\text{Ce}(\text{OH}_2)_9]^{3+}$ species among other hydrated cations. Their calculations was based on the simplified model of a heteronuclear diatomic species, A–B, but such an assumption is not correct. The symmetrical normal mode ν_1 of the CeO₉ skeleton of the $[\text{Ce}(\text{OH}_2)_9]^{3+}$ species reveals that the central cation stays stationary and only the water molecules are involved in the breathing motion.

3.2. Concentration dependent Raman spectra in $\text{Ce}(\text{ClO}_4)_3(\text{aq})$ solutions and the $\text{Ce}(\text{ClO}_4)_3 \cdot 6\text{H}_2\text{O}$ melt

In dilute perchlorate solutions, the formation of contact ion pairs of perchlorate with La^{3+} ,¹⁸ Ce^{3+} , Pr^{3+} , Nd^{3+} and Sm^{3+} is negligible. The breathing modes, ν_1 LnO₉, in these solutions are the ones of the fully hydrated Ln³⁺ ions, the nona-hydrates. Representative of the other rare earth perchlorate solutions, the concentration dependence of the $\text{Ce}(\text{ClO}_4)_3$ solutions will now be discussed. At $\text{Ce}(\text{ClO}_4)_3$ concentrations >1.5 mol L⁻¹, the Raman spectra reveal signs of contact ion pair formation. Raman scattering profiles from 48–1425 cm⁻¹, R_{VV} , R_{VH} and R_{iso} of an aqueous $\text{Ce}(\text{ClO}_4)_3$ solution at 3.118 mol L⁻¹ (mole ratio water to $\text{Ce}(\text{ClO}_4)_3$ = 11.68 : 1) are presented in Fig. 3. In addition to the perchlorate bands, a broad, weak and strongly polarized band at 340 cm⁻¹ is observed, namely, the Ce–O breathing mode. The strong influence of the $\text{Ce}(\text{ClO}_4)_3$ on the water deformation band and its O–H stretching region, especially the perchlorate anion, is given in Fig. S9, ESI† (see ref. 15 and 18).

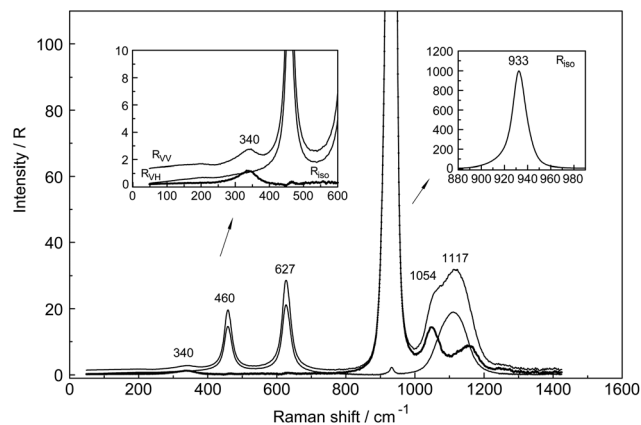


Fig. 3 Raman spectra (R_{VV} , R_{VH} and R_{iso} as slightly thicker line) of a 3.118 mol L⁻¹ $\text{Ce}(\text{ClO}_4)_3$ solution ($R_{\text{w}} = 11.68$) at 22 °C.

In the most concentrated solution at 3.118 mol L⁻¹, the Ce–O breathing mode appears four wavenumbers lower than in the dilute solution (0.202 mol L⁻¹) at 344 cm⁻¹. Furthermore, the band width of the ν_1 Ce–O breathing mode in the most concentrated solution (3.118 mol L⁻¹) broadens by an additional ~17 cm⁻¹ compared to the most dilute solution (0.202 mol L⁻¹) with its fwhh = 50 cm⁻¹. The band profile of the Ce–O breathing mode contains two component bands, one, at 326.5 cm⁻¹ with a fwhh = 79.8 cm⁻¹ containing 59.8% of the whole band area and a component band at 344 cm⁻¹ with a fwhh = 48 cm⁻¹ representing 40.2% of the band area. The component at 326.5 cm⁻¹ represents the Ce–O mode of the partially hydrated Ce³⁺ species while that at 344 cm⁻¹ represents the fully hydrated Ce³⁺ (Fig. S10, ESI†).

The direct contact of ClO_4^- on Ce³⁺ causes marked changes of these ligated perchlorate bands and therefore, the band parameters of these perchlorate bands in $\text{Ce}(\text{ClO}_4)_3$ solution will be considered. The discussion of the perchlorate band parameters shall begin with the most intense perchlorate band, $\nu_1(\text{a}_1)$ ClO_4^- . In a 0.202 mol L⁻¹ $\text{Ce}(\text{ClO}_4)_3$ solution, the $\nu_1(\text{a}_1)$ mode peaks at 932.2 cm⁻¹ and possesses a fwhh at 9.2 cm⁻¹. A 0.404 mol L⁻¹ solution shows a peak position at 932.5 cm⁻¹ with a fwhh at 9.35 cm⁻¹; in a 0.942 mol L⁻¹ solution the band peaks at 932.7 cm⁻¹ and has a fwhh = 9.71 cm⁻¹, and in a solution at 1.889 mol L⁻¹ the band peaks at 932.8 cm⁻¹ and has a fwhh = 10.34 cm⁻¹. Finally, in the solution at 3.118 mol L⁻¹ the $\nu_1(\text{a}_1)$ ClO_4^- band appears at 933.4 cm⁻¹ and has a fwhh at 15.8 cm⁻¹ and is therefore much broader than the band in dilute $\text{NaClO}_4(\text{aq})$ (peak position of $\nu_1(\text{a}_1)$ at 931.5 cm⁻¹ and a fwhh = 7.2 cm⁻¹). A concentration plot of the ν_1 ClO_4^- band profiles in $\text{Ce}(\text{ClO}_4)_3(\text{aq})$ as a function of the solute concentration from 0.202 mol L⁻¹ to the highest concentration at 3.118 mol L⁻¹ is presented in Fig. 4.

In addition, to the intrinsic low frequency shoulder at ~922 cm⁻¹ (Fermi resonance), a broad band at 942 cm⁻¹ emerges in the concentrated $\text{Ce}(\text{ClO}_4)_3$ solutions. Three band components were detected: the first one at 918 cm⁻¹ (fwhh = 26.1 cm⁻¹), the second at 933 cm⁻¹ (fwhh = 12.97 cm⁻¹) and

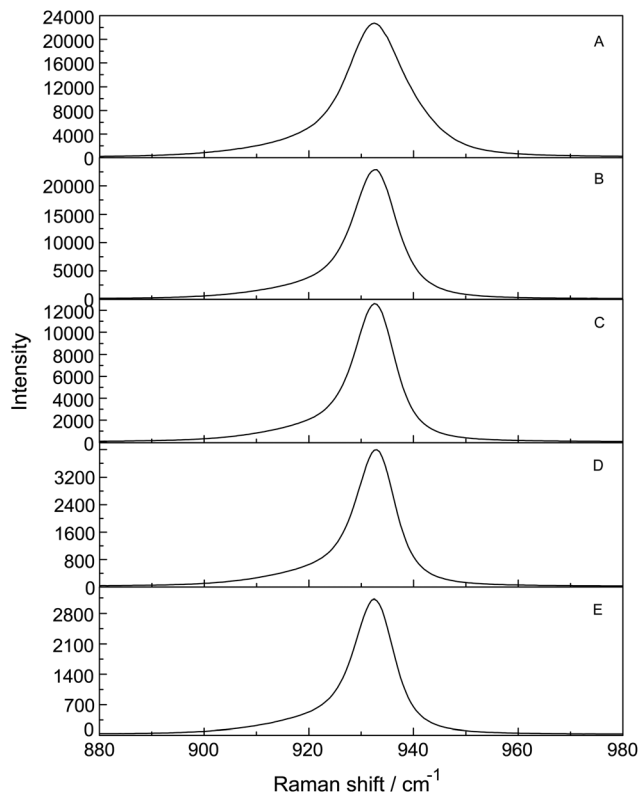


Fig. 4 Concentration plot of the ν_1 ClO_4^- band profiles in $\text{Ce}(\text{ClO}_4)_3(\text{aq})$ as a function of the solute concentration: (A) 3.118 mol L^{-1} ($R_w = 11.68$), (B) 1.886 mol L^{-1} ($R_w = 22.03$), (C) 0.942 mol L^{-1} ($R_w = 51.47$), (D) 0.404 mol L^{-1} ($R_w = 129.14$) and (E) 0.202 mol L^{-1} ($R_w = 268.74$). Note, the very large band width in the most concentrated $\text{Ce}(\text{ClO}_4)_3$ solution (A).

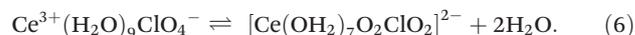
the third at 942 cm^{-1} (fwhh = 13.95 cm^{-1}). The first two bands of the $\nu_1(a_1)$ ClO_4^- profile also appear in the fully hydrated ClO_4^- , albeit much broader, while the third band component at 942 cm^{-1} is a new component. This finding clearly indicates two different sites for the ClO_4^- ; one in the outer-sphere position and the other constituting the contact ion pair binding directly to Ce^{3+} . At such a high concentration state, the ClO_4^- has to occur in an outer-sphere ion pair, $\text{Ce}^{3+}(\text{OH}_2)\text{ClO}_4^-$.

The other three perchlorate bands also show large deviations from the ones found in dilute $\text{NaClO}_4(\text{aq})$ as explained above. The antisymmetric stretch, $\nu_3(f_2)\text{ClO}_4^-$, appears with a band width of 128 cm^{-1} compared to 65 cm^{-1} in fully hydrated $\text{ClO}_4^-(\text{aq})$. Several broad unresolved band components were observed in the polarized band profile of $\nu_3(f_2)$ ClO_4^- which was fitted with four bands with components at 1051 cm^{-1} (fwhh = 45.8 cm^{-1}), 1102 cm^{-1} (fwhh = 81.8 cm^{-1}), 1133.4 cm^{-1} (fwhh = 61 cm^{-1}) and 1153.5 cm^{-1} (fwhh = 51.7 cm^{-1}). Two weak and broad band components were detected in the isotropic scattering profile at 1050 cm^{-1} and at 1156 cm^{-1} . These isotropic band contributions can only be explained by reduction of the T_d ClO_4^- symmetry due to direct bonding on the Ce^{3+} ion.

The deformation modes in the most concentrated solution also show large deviations from the one in dilute $\text{ClO}_4^-(\text{aq})$.

The first broad deformation mode $\nu_2(e)$ at 460 cm^{-1} shows a high frequency shoulder at *ca.* 470 cm^{-1} and the second deformation mode $\nu_4(f_2)$ at 627 cm^{-1} is also much broader and slightly asymmetric compared to the one in the fully hydrated $\text{ClO}_4^-(\text{aq})$ spectrum (see above).

In the most dilute solution, with its 269 water molecules per $\text{Ce}(\text{ClO}_4)_3$, the water content is large enough to completely hydrate all ions. In such a dilute solution no inner-sphere ion pairs are formed. Although the perchlorate ion is known as a non-complex forming anion, contact ion pair formation, however, becomes more and more likely with an increase in solute concentration and a shrinking amount of water. In the 3.118 mol L^{-1} solution, only 11.68 water molecules are available which are not enough to fully hydrate all ions. Inevitably, ion-pair formation must occur. The ion pair formation between $\text{Ce}^{3+}(\text{aq})$ and $\text{ClO}_4^-(\text{aq})$ most likely occurs in a step-wise equilibrium process with the outer-outer sphere and outer-sphere ion pairs, $\text{Ce}^{3+}(\text{H}_2\text{O})_2\text{ClO}_4^-$ and $\text{Ce}^{3+}(\text{H}_2\text{O})\text{ClO}_4^-$, respectively. In the most concentrated solution, *ca.* 20% contact ion pairs are formed which are in equilibrium with the outer-sphere ion pairs of the formula: $\{\text{Ce}^{3+}(\text{H}_2\text{O})_9\text{ClO}_4^-\}$. The equilibrium in the concentrated solution state may be formulated according to:



To summarize, the perchlorate ion penetrates the flexible first hydration shell of Ce^{3+} in concentrated solutions in contrast to $\text{Al}(\text{ClO}_4)_3$ solutions, where perchlorate does not penetrate into the first hydration shell of Al^{3+} .^{25,26} The hydration shell of $[\text{Al}(\text{OH}_2)_6]^{3+}$ is inert.²⁶ In a $\text{Ce}(\text{ClO}_4)_3$ hydrate melt with a shortage of water, contact ion pair formation should be pronounced. Such a hydrate melt will be discussed in the following section.

In a $\text{Ce}(\text{ClO}_4)_3 \cdot 6\text{H}_2\text{O}$ melt at $161 \text{ }^\circ\text{C}$, shown in Fig. 5, the deviations of the ligated perchlorate bands are most pro-

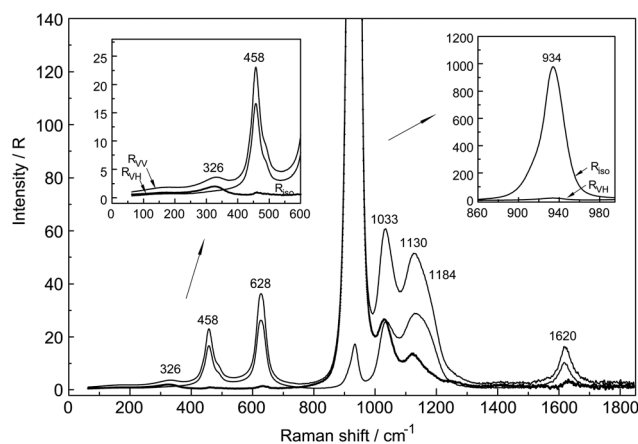


Fig. 5 Raman scattering profiles (R_{VV} , R_{VH} and R_{iso} as slightly thicker line) of a $\text{Ce}(\text{ClO}_4)_3$ hydrate melt of the composition $\text{Ce}(\text{ClO}_4)_3$ plus $6\text{H}_2\text{O}$ at $161 \text{ }^\circ\text{C}$. The left inset shows the scattering profile in the terahertz region in detail. The right inset shows the isotropic and anisotropic scattering profiles of the ν_1 ClO_4^- band at full scale.

nounced and are compared to the $\text{Ce}(\text{ClO}_4)_3$ solution state. The Ce–O breathing mode will be discussed below.

The bands of the ligated ClO_4^- in the melt are broad and show distinct new band features. The deformation mode of $\nu_2(\text{e}) \text{ClO}_4^-$ at 458 cm^{-1} , for instance, splits into two broad components; one at 457.5 cm^{-1} (fwhh = 35.5 cm^{-1}) and a second positioned at 489.7 cm^{-1} (fwhh = 26 cm^{-1}). The $\nu_4(\text{f}_2) \text{ClO}_4^-$ deformation mode, also broad and with an asymmetric profile peaks at 628 cm^{-1} . The whole band complex shows three components: a first one at 586 cm^{-1} (fwhh = 35.3 cm^{-1}), a second at 621.9 cm^{-1} (fwhh = 24.7 cm^{-1}) and a third at 635.2 cm^{-1} (fwhh = 28.1 cm^{-1}). The Raman scattering profiles in *R*-format in the lower part of the wavenumber region from $60\text{--}800 \text{ cm}^{-1}$ showing both deformation modes of ClO_4^- are presented in greater detail in Fig. S11A, ESI†. The band fit results from the polarized scattering profiles for $\nu_2(\text{e}) \text{ClO}_4^-$ and $\nu_4(\text{f}_2) \text{ClO}_4^-$ such as the sum curve of the band fit and the component bands together with the measured profiles are presented in Fig. S11B and S11C, respectively (ESI†). The $\nu_1(\text{a}_1) \text{ClO}_4^-$ band, the perchlorate symmetric stretch with the highest intensity in the Raman spectrum located at 934 cm^{-1} and its fwhh at 24.5 cm^{-1} appears dramatically broadened compared to the dilute solution state (fwhh = $\sim 7.8 \text{ cm}^{-1}$). The band profile shows an asymmetric band contour at 941 cm^{-1} in addition to the asymmetry stemming from the Fermi resonance component at 914 cm^{-1} . The Fermi resonance band, however, also appears in the spectrum of the fully hydrated $\text{ClO}_4^-(\text{aq})$ as was discussed in detail above. The component band at 941 cm^{-1} stems clearly from the ligated ClO_4^- of the inner-sphere ion pairs. The band fit results for the isotropic $\nu_1(\text{a}_1) \text{ClO}_4^-$ profile in *R*-format is given in Fig. S12, ESI†. The antisymmetric Cl–O stretching mode, $\nu_3(\text{f}_2) \text{ClO}_4^-$, is very broad compared to the one in the fully hydrated $\text{ClO}_4^-(\text{aq})$ and the band complex shows clearly two band components and a pronounced asymmetry at higher wavenumbers. These bands are not only visible in the polarized or depolarized scattering but also in the isotropic scattering with its components at 1033 cm^{-1} and 1130 cm^{-1} and a broad shoulder at 1184 cm^{-1} (see Fig. S13, ESI†). In contrast, in dilute $\text{ClO}_4^-(\text{aq})$ the band peaks at 1106 cm^{-1} , appears much smaller and is completely depolarized.

Finally, the Ce–O breathing mode normally positioned at 344 cm^{-1} shifts to 326 cm^{-1} and broadens considerably (fwhh = 81 cm^{-1}). The band was fitted with two components at 306 cm^{-1} (fwhh = 65 cm^{-1}) and at 332.8 cm^{-1} (fwhh = 56 cm^{-1}). Furthermore, a small isotropic component at 159 cm^{-1} is detectable (see Fig. S11A, ESI†).

All these spectroscopic features clearly show that the symmetry of the ligated ClO_4^- and its geometry are considerably altered due to the direct coordination to Ce^{3+} . Consequently, the vibrational bands lose their degeneracy and shift. The monodentate binding of one of the four oxygen atoms of the perchlorate will reduce the symmetry of the ligated ClO_4^- from T_d to C_{3v} . Bidentate binding of two of the oxygen atoms of ClO_4^- to Ce^{3+} will reduce the symmetry further to C_{2v} (correlation table of T_d symmetry with C_{3v} and C_{2v} see ref. 27). The

most likely type of coordination of the perchlorate, however, will be an asymmetric bidentate binding with the two ligated oxygen atoms with different Ce–O bond distances. This would lead then to symmetry C_1 . The two isotropic components in the antisymmetric Cl–O stretching region, mentioned above, are an indication. The Ce^{3+} -perchlorate inner-sphere ion pairs are the dominate species in the hydrate melt at $161 \text{ }^\circ\text{C}$ in equilibrium with the outer-sphere species, $\{\text{Ce}^{3+}(\text{H}_2\text{O})_9\text{ClO}_4^-\}$.

The results of a combined X-ray scattering and ^{35}Cl NMR spectroscopic study on $\text{Ce}(\text{ClO}_4)_3(\text{aq})$ and on $\text{Mg}(\text{ClO}_4)_2(\text{aq})$ verify the formation of contact ion pairs in Ce^{3+} solutions depending on the solute concentration.^{28,29} In $\text{Mg}(\text{ClO}_4)_2$ solutions, however, no contact ion-pairs could be verified. Again, recent Raman data support this finding and confirm that the first hydration sphere of Mg^{2+} is inert for ClO_4^- penetration.³⁰ The Raman spectroscopic findings confirm the results of the combined X-ray scattering technique and ^{35}Cl NMR spectroscopy. Furthermore, a recent study on aqueous La^{3+} perchlorate solutions confirmed the labile hydration structure of the $\text{La}^{3+}(\text{aq})$ and the formation of $\text{La}^{3+}\text{--ClO}_4^-$ inner-sphere ion pairs in concentrated solutions.¹⁸

3.3. CeCl_3 solutions

From thermodynamic measurements, it is known that Ce^{3+} forms weak chloro-complexes/ion-pairs.^{31,32} As a model system for the strongly coloured praseodymium- and neodymium-chloride solutions, aqueous CeCl_3 solutions at 2.167 mol L^{-1} ($R_w = 23.61$), 1.083 mol L^{-1} ($R_w = 49.23$) and 0.270 mol L^{-1} ($R_w = 203.1$) were studied Raman spectroscopically. In addition, a ternary solution, $\text{CeCl}_3\text{--HCl--H}_2\text{O}$, was also investigated. The Raman scattering profiles of a 2.167 mol L^{-1} CeCl_3 solution ($R_w = 23.61$) are presented in Fig. 6 in the wavenumber range from $75\text{--}700 \text{ cm}^{-1}$ in *R*-format and that of the solution at 0.270 mol L^{-1} in Fig. 7. The Ce–O stretching mode in the 2.167 mol L^{-1} solution is down shifted and appears at 341 cm^{-1} . A broad isotropic component at 201 cm^{-1} and an unresolved broad feature at 245 cm^{-1} are also observed. These findings are clear evidence that Cl^- has penetrated into the first hydration shell of Ce^{3+} and partially hydrated Ce^{3+} chloro-complex species formulated as $[\text{Ce}(\text{OH}_2)_{9-n}\text{Cl}_n]^{+3-n}$ with $n = 1, 2$ are formed. The second isotropic component at 201 cm^{-1} is assigned to the restricted translation band of water of its $\text{O--H}\cdots\text{O}/\text{Cl}^-$ units and the third broad feature to the $\nu \text{Ce}^{3+}\text{--Cl}^-$ stretching mode(s) of the Ce^{3+} -chloro-complex species. With dilution, the Ce–O mode shifts to higher wavenumbers. For a 2.167 mol L^{-1} in which the mole ratio of solute to water is 1 to 23.61, the Ce–O breathing mode appears at 341 cm^{-1} and at a concentration at 1.013 mol L^{-1} ($R_w = 52.5$) appears at 342 cm^{-1} . The Raman spectral scattering profiles of a 0.270 mol L^{-1} ($R_w = 203.1$) in Fig. 7 show the Ce–O breathing mode at 344 cm^{-1} and the chloro-complex species almost diminished. These Raman spectroscopic results demonstrate that with dilution the chloro-complex species disappear rapidly. Extrapolation of our Raman data leads to the conclusion that in $\text{CeCl}_3(\text{aq}) < 0.1 \text{ mol L}^{-1}$ the Ce^{3+} ion is fully hydrated. These findings show that Ce^{3+} forms weak complexes with Cl^- .

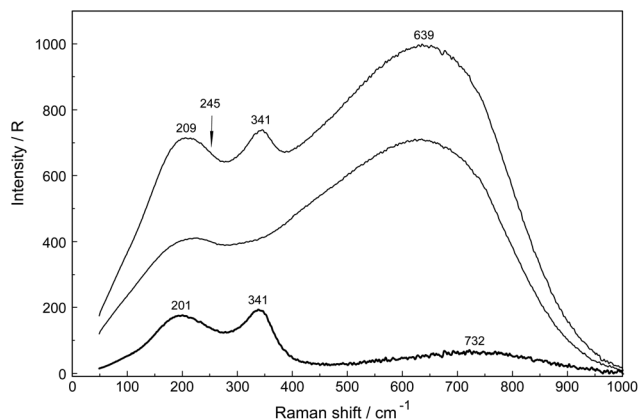


Fig. 6 The Raman scattering profiles in *R*-format (from top to bottom: R_{VV} , R_{VH} and R_{iso}) of a 2.167 mol L⁻¹ CeCl₃ solution ($R_w = 23.61$) at 22 °C. The wavenumbers range from 50 to 1000 cm⁻¹. The very broad band at 639 cm⁻¹, considering the R_{VV} scattering, represents the librational modes of water. In the terahertz region, below 400 cm⁻¹, the following modes show: 341 cm⁻¹, ν_1 the Ce–O breathing mode and at 209 cm⁻¹ the restricted translation mode of water of the O–H...O/Cl⁻ units. Considering the isotropic scattering the restricted translational water band peaks at 201 cm⁻¹ but also contains broad and unresolved feature at ca. 245 cm⁻¹ indicated by arrow. These broad, unresolved features represent the Ce–Cl stretching band(s). In the isotropic scattering the very broad band at 732 cm⁻¹ is due to the water librations.

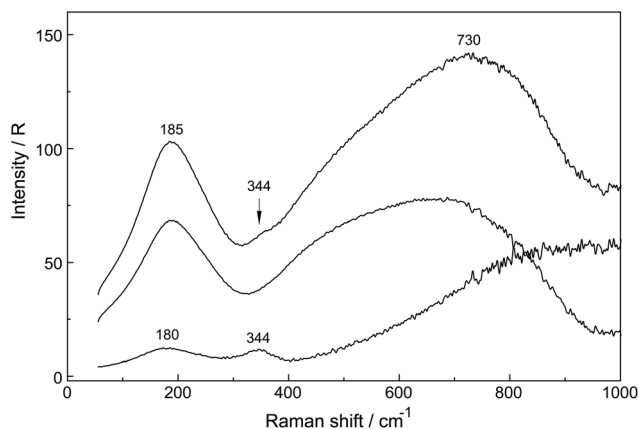


Fig. 7 Raman scattering profiles of a 0.270 mol L⁻¹ CeCl₃ solution ($R_w = 203.1$) in the wavenumber region from 50–1000 cm⁻¹. *R*-Scattering profiles (from top to bottom: R_{VV} , R_{VH} and R_{iso}) at 22 °C. The very broad band at 730 cm⁻¹ (R_{iso} : ~910 cm⁻¹) is due to water librations. In the terahertz region, below 400 cm⁻¹, the following modes in the R_{iso} scattering show the ν_1 Ce–O breathing mode at 344 cm⁻¹ and at 185 cm⁻¹ (R_{iso} : 180 cm⁻¹) the restricted translational band of water of the O–H...O units.

To further verify chloro-complex formation in CeCl₃(aq), a ternary solution, CeCl₃–HCl–H₂O, was studied. In Fig. 8 the isotropic scattering of a CeCl₃–HCl solution with a CeCl₃ concentration at 2.03 mol L⁻¹ and 4.0 mol L⁻¹ HCl is shown. From the isotropic spectrum of CeCl₃(aq) at 2.03 mol L⁻¹ plus 4.0 mol L⁻¹ HCl the isotropic scattering profile of a 4 mol L⁻¹ HCl(aq) was subtracted and the difference spectrum reveals a

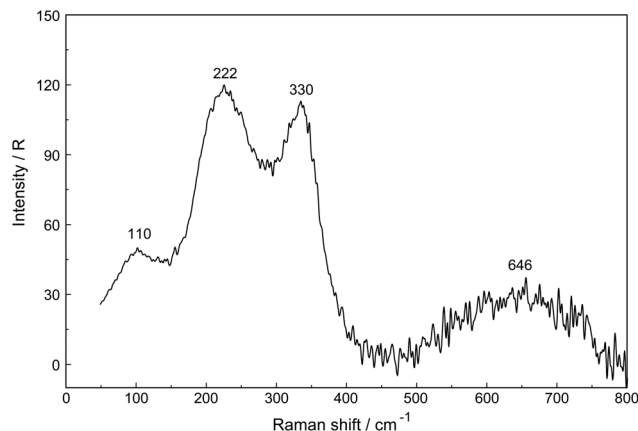
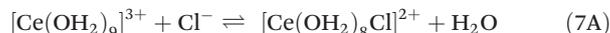


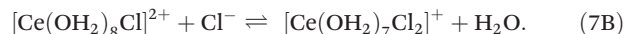
Fig. 8 The isotropic Raman scattering profile (R_{iso}) of a 2.167 mol L⁻¹ CeCl₃ solution with additional 4.01 mol L⁻¹ HCl added at 22 °C. The wavenumber range is from 50 to 800 cm⁻¹. The band at 330 cm⁻¹ represents the Ce–O mode of the partially hydrated chloro – complex species of Ce³⁺, [Ce(OH)₂]_{9-n}Cl_n⁺³⁻ⁿ with $n = 1$ and/or 2. The broader band complex at 222 cm⁻¹ is assigned to the Ce³⁺–Cl⁻ modes as well as the band at 110 cm⁻¹ of the chloro-complex species. The very broad band at 646 cm⁻¹ represents the librational modes of the water in this ternary solution.

broad band at 329 cm⁻¹ and one at 222 cm⁻¹ and a smaller scattering contribution at 101 cm⁻¹ (Fig. 8).

The marked shift of the isotropic band of the Ce–O breathing mode at 341 cm⁻¹ in a 2.167 mol L⁻¹ CeCl₃ solution without added HCl (Fig. 6) compared to the peak position at 329 cm⁻¹ in CeCl₃ plus HCl (Fig. 8) shows the extensive formation of chloro-complex(es). A stepwise formation may be formulated according to:



and with an increase in Cl⁻ a second chloro-complex may be formed according to eqn (7B):



The estimated value of the $\log \beta_1$ value for eqn (7A) equal to ~0.1 reveals the weak nature of the chloro-complex in CeCl₃(aq) at 22 °C. Thermodynamic data on the chloro-complex formation in CeCl₃(aq) confirm the weak nature of the complexes and values for the equilibrium constants for reactions (7A) and (7B) may be found in ref. 31 and 32.

The existence of a chloro-complex species in concentrated LaCl₃ solutions using Raman spectroscopy in the terahertz region was presented recently.¹⁸ The results on LaCl₃ solutions from dilute to concentrated ones¹⁸ are quite similar to the recent findings on CeCl₃ solutions. The chloride ion penetrates the flexible first hydration shell of La³⁺ and Ce³⁺ and pushes out water. With dilution, the weak chloro-complexes disappear and fully hydrated La³⁺ resp. Ce³⁺ ions could be detected. In contrast, in concentrated AlCl₃ solutions, Cl⁻ does not penetrate into the first hydration shell of Al³⁺.^{25,26} The hydration shell of [Al(OH)₂]₆³⁺ is quite inert²⁶ and the

symmetric stretching mode of the ν_1 AlO_6 skeleton at 525 cm^{-1} could be observed in the whole concentration series of $\text{AlCl}_3(\text{aq})$ (0.5 to 3.14 mol L^{-1}).

The results of an extensive EXAFS study on 0.1 and 0.01 mol L^{-1} La^{3+} , Ce^{3+} and Nd^{3+} – solutions in 0.20 mol L^{-1} HCl and with 14 mol L^{-1} LiCl are especially instructive.³³ (Ref. 33 also contains data on heavy rare earth and actinide ions.) Allen and co-workers³³ showed convincingly that in solutions with low chloride concentrations the Ln–O bond distances for Ln^{3+} ($\text{Ln} = \text{La}, \text{Ce}$ and Nd) and coordination numbers equal to ~ 9 are consistent with fully hydrated La^{3+} , Ce^{3+} and Nd^{3+} ions, the nona-hydrates. In solutions with an excess of LiCl , it was demonstrated that inner sphere chloro-complexation takes place together with a loss of water.³² The average chloride coordination numbers and Ln–Cl bond lengths for La^{3+} , Ce^{3+} and Nd^{3+} were also given.³³ In a recent combined EXAFS and XRD study³⁴ ion pair formation was reported in a 1.0 mol kg^{-1} LaCl_3 solution. Our results of concentration dependent Raman profiles on $\text{CeCl}_3(\text{aq})$ and the results on $\text{LaCl}_3(\text{aq})$ ¹⁸ confirm the data of these structural studies.^{33,34}

To summarize, the $[\text{Ce}(\text{OH}_2)_{9-n}\text{Cl}_n]^{3-n}$ modes in chloride solutions could be detected and formation of weak chloro-complexes with Ce^{3+} verified. In dilute solutions ($c < 0.1\text{ mol L}^{-1}$) the chloro-complex species disappeared upon dilution and $[\text{Ce}(\text{OH}_2)_9]^{3+}$ and $\text{Cl}^-(\text{aq})$ are formed. The chloro-complex formation may be one reason for the data scatter of the recently published Ce–O bond distances and coordination numbers presented for $\text{Ce}^{3+}(\text{aq})$ and other rare earth chloride systems.^{33,34} In recent experimental structural studies, it was observed that inner-sphere chloro-complex species are formed in aqueous LnCl_3 solution ($\text{Ln} = \text{La}, \text{Ce}$ and Nd) with high chloride concentrations while in dilute solutions, fully hydrated ions exist.^{33,34}

4. Conclusions

Raman measurements on dilute aqueous $\text{La}(\text{ClO}_4)_3$, $\text{Ce}(\text{ClO}_4)_3$, $\text{Pr}(\text{ClO}_4)_3$, $\text{Nd}(\text{ClO}_4)_3$ and $\text{Sm}(\text{ClO}_4)_3$ solutions have been carried out. In these solutions, strongly polarized modes at 343 cm^{-1} , 344 cm^{-1} , 347 cm^{-1} , 352 cm^{-1} and 363 cm^{-1} were detected and assigned to the breathing modes, ν_1 Ln–O of the nona-hydrates $[\text{La}(\text{H}_2\text{O})_9]^{3+}$, $[\text{Ce}(\text{H}_2\text{O})_9]^{3+}$, $[\text{Pr}(\text{H}_2\text{O})_9]^{3+}$, $[\text{Nd}(\text{H}_2\text{O})_9]^{3+}$ and $[\text{Sm}(\text{H}_2\text{O})_9]^{3+}$. The force constants of these Ln–O breathing modes were calculated from these data. In the dilute perchlorate solutions, these species represent the fully hydrated $[\text{Ln}(\text{OH}_2)_9]^{3+}$ ions. The calculated force constants of the nona-hydrates of $[\text{La}(\text{H}_2\text{O})_9]^{3+}$, $[\text{Ce}(\text{H}_2\text{O})_9]^{3+}$, $[\text{Pr}(\text{H}_2\text{O})_9]^{3+}$, $[\text{Nd}(\text{H}_2\text{O})_9]^{3+}$ and $[\text{Sm}(\text{H}_2\text{O})_9]^{3+}$ strengthen with the corresponding decrease in the Ln–O bond distances.

In $\text{Ce}(\text{ClO}_4)_3$ in heavy water, the Ce–O breathing mode shifts to 326 cm^{-1} for the deuterated species $[\text{Ce}(\text{OD}_2)_9]^{3+}$ as a result of the isotope effect by changing from H_2O to D_2O .

As a typical example of these lanthanide perchlorate solutions, higher concentrated aqueous $\text{Ce}(\text{ClO}_4)_3$ solutions were studied. In the highest concentrated $\text{Ce}(\text{ClO}_4)_3$ solution,

3.118 mol L^{-1} , contact ion pairs between Ce^{3+} and ClO_4^- were detected. In a hydrate melt of $\text{Ce}(\text{ClO}_4)_3$ plus $6\text{H}_2\text{O}$, measured at $161\text{ }^\circ\text{C}$, the contact ion pairs dominate the spectrum. The bands of the ligated ClO_4^- were characterized as well as the ν_1 Ce–O breathing mode of the partially hydrated Ce^{3+} species, $[\text{Ce}(\text{H}_2\text{O})_7\text{O}_2\text{ClO}_2]^{2+}$.

In CeCl_3 solutions, Cl^- penetrates the first hydration sphere of $\text{Ce}^{3+}(\text{aq})$ and weak chloro-complexes are formed. However, the chloro complexes disappear rapidly upon dilution and at a concentration $< 0.1\text{ mol L}^{-1}$ the chloro-complexes have almost disappeared. These Raman spectroscopic findings were substantiated by recently published Raman and EXAFS results.^{18,33,34}

Acknowledgements

WWR and GI thank Frau B. Ostermayr for her skilful technical assistance.

References

- C.-H. Huang and Z. Bian, in *Introduction in Rare Earth Coordination Chemistry: Fundamentals and Applications*, ed. C.-H. Huang, Wiley, Singapore, 2010.
- N. A. Piro, J. R. Robinson, P. J. Walsh and E. J. Schelter, *Coord. Chem. Rev.*, 2014, **260**, 21–36.
- Y. Marcus, *Biophys. Chem.*, 1994, **51**, 111–127.
- J. Burgess, *Ions in Solution: Basic Principles of Chemical Interactions*, Ellis Horwood, Chichester/Halsted Press, New York, 1988.
- P. D'Angelo, S. De Panfilis, A. Filipponi and I. Persson, *Chem. – Eur. J.*, 2008, **14**, 3045–3055.
- P. D'Angelo and R. Spezia, *Chem. – Eur. J.*, 2012, **18**, 11162–11178.
- H. Ohtaki and T. Radnai, *Chem. Rev.*, 1993, **93**, 1157–1204.
- I. Persson, P. D'Angelo, S. De Panfilis, M. Sandström and L. Eriksson, *Chem. – Eur. J.*, 2008, **14**, 3056–3066.
- M. Duvail, P. Vitorge and R. Spezia, *J. Chem. Phys.*, 2009, **130**, 104501.
- P. D'Angelo, A. Zitolo, V. Migliorati, G. Chillemi, M. Duvail, P. Vitorge, S. Abadie and R. Spezia, *Inorg. Chem.*, 2011, **50**, 4572–4579.
- J. L. Pascal and F. Favier, *Coord. Chem. Rev.*, 1998, **178–180**, 865–902.
- L. Johansson, *Coord. Chem. Rev.*, 1974, **12**, 241–261.
- P. Krumholz, *J. Phys. Chem.*, 1959, **83**, 2038–2042.
- H. Kanno and J. Hiraishi, *J. Phys. Chem.*, 1984, **88**, 2787–2792.
- W. W. Rudolph and G. Irmer, *Dalton Trans.*, 2013, **42**, 3919–3935.
- W. W. Rudolph and G. Irmer, *Dalton Trans.*, 2015, **44**, 18492–18505.
- W. W. Rudolph and G. Irmer, *Appl. Spectrosc.*, 2007, **61**, 1312–1327.

- 18 W. W. Rudolph and G. Irmer, *Dalton Trans.*, 2015, **44**, 295–305.
- 19 A. I. Vogel, *A Text-Book of Quantitative Inorganic Analysis*, Longman, London, 3rd edn, 1961.
- 20 F. H. Spedding, M. J. Pikal and B. O. Ayers, *J. Phys. Chem.*, 1966, **70**, 2440–2449.
- 21 C. K. Jørgensen and J. S. Brinen, *Mol. Phys.*, 1963, **6**, 629–630.
- 22 K. Binnemans and C. Görller-Walrand, *Chem. Phys. Lett.*, 1995, **235**, 163–174.
- 23 W. W. Rudolph, *Z. Phys. Chem.*, 1996, **194**, 73–95.
- 24 O. M. D. Lutz, T. S. Hofer, B. R. Randolph and B. M. Rode, *Chem. Phys. Lett.*, 2012, **539/540**, 50–53.
- 25 W. W. Rudolph, *Z. Phys. Chem.*, 1989, **270**, 1121–1134.
- 26 W. W. Rudolph, R. Mason and C. C. Pye, *Phys. Chem. Chem. Phys.*, 2000, **2**, 5030–5040.
- 27 W. W. Rudolph and S. Schönherr, *Z. Phys. Chem.*, 1991, **172**, 31–48.
- 28 R. Caminiti, G. Cerioni, G. Crisponi and P. Cucca, *Z. Naturforsch., A: Phys. Sci.*, 1988, **43**, 317–325.
- 29 R. Caminiti, P. Cucca and A. D'Andrea, *Z. Naturforsch., A: Phys. Phys. Chem. Kosmophys.*, 1983, **38**, 533–539.
- 30 W. W. Rudolph, G. Irmer and G. T. Hefter, *Phys. Chem. Chem. Phys.*, 2003, **5**, 5253–5261.
- 31 S. A. Wood, *Chem. Geol.*, 1990, **82**, 159–186.
- 32 J. Schijf and R. H. Byrne, *Geochim. Cosmochim. Acta*, 2004, **68**, 2825–2837.
- 33 P. G. Allen, J. J. Bucher, D. K. Shuh, N. M. Edelstein and I. Craig, *Inorg. Chem.*, 2000, **39**, 595–601.
- 34 S. Díaz-Moreno, S. Ramos and D. T. Bowron, *J. Phys. Chem. A*, 2011, **115**(24), 6575–6581.